DOI: 10.61782/fa.2025.0489

INTERPOLATION OF MODAL DISPLACEMENT IN THIN PLATES USING PHYSICS-INFORMED NEURAL NETWORKS

Raffaele Malvermi **Francesco Zese** **Mirco Pezzoli**
Fabio Antonacci **Augusto Sarti**
Dipartimento di Elettronica, Informazione e Bioingegneria, Politecnico di Milano, Milan, Italy

ABSTRACT

Predicting vibrational displacement fields and mode shapes in thin plates is crucial for various engineering applications, particularly in the acoustic characterization of musical instrument soundboards. Traditional methods are limited by high computational costs or dense measurement requirements e.g., Finite Element Analysis (FEA). This study introduces a Physics-Informed Neural Network (PINN) approach to reconstruct displacement fields using sparse data. The PINN integrates the Kirchhoff plate equation into its training process, enabling accurate predictions even in data-sparse regions. The model was validated using COMSOL simulations of a thin rectangular plate, with material properties resembling a violin soundboard. Its performance was compared to Radial Basis Function (RBF) interpolation and data-driven neural networks. The PINN consistently outperformed the considered baselines, achieving robust results with minimal data, particularly for higher resonant frequencies where other methods fail.

Keywords: *physics-informed neural network, structural analysis, interpolation, modal analysis*

1. INTRODUCTION

Accurately predicting displacement fields and mode-shapes in vibrating structures is of fundamental importance across various engineering fields, including aerospace, structural mechanics, and acoustics.

In structural mechanics, accurately predicting the displacement fields and mode shapes of vibrating structures is a fundamental task across a wide range of applications, from aerospace and civil engineering to the acoustic design of musical instruments. In particular, the acoustic characterization of thin wooden plates is fundamental for designing and tuning stringed instruments, as the vibrational behavior of the soundboard directly influences sound quality [1]. Classical Experimental Modal Analysis (EMA) relies on multiple spatially-distributed measurements to extract modal parameters such as natural frequencies, damping ratios, and mode shapes from the acquired data [2–4]. However, practical constraints often lead to suboptimal sparse sensor data. For instance, in musical instruments, parts of the soundboard may be inaccessible due to physical obstructions such as the fingerboard, making a full-field measurement challenging.

Traditional approaches, such as Finite Element Analysis (FEA) [5, 6] and Nearfield Acoustic Holography (NAH) [7], have been employed to predict vibrational behavior. While FEA is capable of providing detailed insight into complex vibrational phenomena, its computational cost and difficulties in modeling intricate geometries limit its practical use. Conversely, NAH requires a dense grid of measurements to yield reliable reconstructions, which is not always feasible.

To overcome the limitations imposed by limited data, different works have investigated sparse optimization techniques to interpolate or reconstruct the full modal shapes from limited data [8, 9]. Compressed Sensing [8] have been employed in [10] to synthesize plate impulse responses as sparse combinations of basis functions, i.e., plane waves, thereby effectively bridging the gap between

*Corresponding author: mirco.pezzoli@polimi.it.

coarse measurements and the desired continuous field. A different approach in [9] integrates sparse regularization decomposing the available measurements into a summation of resonance curves and fitting them with Finite Element Analysis (FEA) mode shapes.

More recently, machine learning emerged as an effective solution in various fields including the design of musical instruments [11, 12], acoustics [13, 14], and, structural analysis [15]. In particular, deep learning has been proposed for the interpolation of vibrational data. A first approach for the so-called super-resolution of modal shapes has been introduced in [16] exploiting a CNN autoencoder trained on ideal rectangular plates. The usage of convolutional autoencoders has been further investigated in [17], which proposes a U-Net [18] architecure for the interpolation of frequency response functions (FRFs). Although effective, the methods in [16,17] employ customary supervised training for which an extensive dataset is required in order to train the models. This represents a limitation for generalization to different objects and real measurements, since training data set are generally synthetic and tailored to a specific object geometry or material parameters.

In order to overcome the need of a training data set in [19] a deep prior approach [20] has been proposed. Through a per-element training, the method in [19] allows one to reconstruct FRFs starting from a limited set of measurements. In fact, deep prior models solve inverse problems such as the upsampling of data points exploiting the inherent regularization given by the adopted neural network structure [21–23]. One main limitation of the deep prior approach is that it does not exploit further a priori-information on the problem under analysis. As a matter of fact, regularization strategies based on the physics of the vibrating system could be ideally exploited.

Therefore, in this work, we propose the adoption of a physics-informed neural network (PINN) [24] for the reconstruction of the displacement field. PINNs emerged as an effective solution for solving several ill-posed problems in vibroacoustics [25, 26] including upsampling of sound field [27–30] and NAH [26, 31]. In fact, PINNs are design to promote solutions that fulfill the governing equations of physical systems, typically involving partial differential equations (PDE), in order to guide the learning of the network. This allows the network to obtain physically meaningful solutions, while eliminating the need of large training sets to learn the underlying behaviour of the system.

Therefore, we adopted a physics-informed SIREN [32], a multilayer perceptron with sinusoidal activations, that is able to provide an implicit representation of the physical quantity and proved to be an effective architecture in several problems [28, 29] akin to modal shape interpolation. We train the PINN with a physics loss implementing the Kirchoff plate equation in order to regularize the predictions. This implicit representation enables the continuous reconstruction of the displacement across the entire domain, allowing the prediction of the displacement at any point, even in regions where no direct data points are available. We evaluated the proposed method against two baseline approaches: Radial Basis Function (RBF) interpolation [33, 34] and a data-driven neural network without physics loss. The results show the superior performance of the PINN with respect to the adopted solutions, suggesting promising adoption of physics-informed SIREN in the context of vibroacoustics.

2. PROPOSED METHOD

2.1 Problem formulation

Let us consider a set of measurements taken at N discrete points $\{\boldsymbol{r}_i = (x_i, y_i)\}_{i=1}^{N}$ over the surface of a thin plate e.g., the sound board of a violin or guitar, capturing the corresponding displacement values at M resonance frequencies $\{\omega_m\}_{m=1}^{M}$. The acquired measurements yield a dataset of the form:

$$\mathcal{D} = \{(\boldsymbol{r}_i, w_i^m)\}, \quad \begin{matrix} i = 1, \ldots, N, \\ m = 1, \ldots, M, \end{matrix} \tag{1}$$

where w_i^m represents the transverse displacement of the plate at the ith spatial point $\boldsymbol{r}_i = (x_i, y_i)$ for the resonant frequency ω_m. Each resonant frequency ω_m corresponds to a different mode shape of the vibrating plate, capturing the distinct patterns of deformation that occur at specific frequencies. The objective is to interpolate the displacement values across the entire surface of the plate, denoted as Ω. Given $\mathcal{D}$, we aim at finding a function that represents the plate displacement $w(\cdot)$ over the entire surface Ω based on the limited number of observation such that

$$\hat{w}(\boldsymbol{r}, \omega_m) = \mathcal{F}(\boldsymbol{\Theta}, \boldsymbol{r}, \omega_m), \tag{2}$$

where $\boldsymbol{\Theta}$ is the set of learnable parameters of the function $\mathcal{F}$. Typically, the solution to the problem in (4) is found through an optimization problem design to determine the

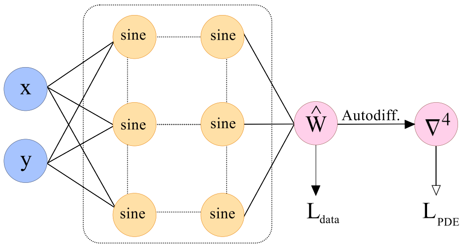

Figure 1. PINN architecture scheme, where the input is the spatial domain represented by the Cartesian coordinates x and y. In SIREN architecture, the sine function is used as the activation function. The output representing the plate displacement is used to compute the data loss and then is differentiated with respect to the inputs to implement the physics loss.

optimal parameters as

$$\hat{\mathbf{\Theta}}_{\text{opt}} = \arg\min_{\mathbf{\Theta}} \sum_i \sum_m \left(|\hat{w}(\mathbf{\Theta}, \boldsymbol{r}_i, \omega_m) - w(\boldsymbol{r}_i, \omega_m)|^2\right) \quad \text{s.t.} \quad \mathcal{R}(\mathbf{\Theta}, \boldsymbol{r}), \tag{3}$$

where $\mathcal{R}(\cdot)$ is a regularization term, designed in order to retrieve meaningful solutions and avoid overfitting.

2.2 PINN for modal interpolation

Building on the problem formulation presented in the previous section, we propose the adoption of a PINN to perform continuous reconstruction of the displacement field. Thus the estimation in (4) becomes

$$\hat{\mathbf{w}}(\boldsymbol{r}) = \mathcal{N}(\mathbf{\Theta}, \boldsymbol{r}), \tag{4}$$

where $\hat{\mathbf{w}}(\boldsymbol{r}) \in \mathbb{C}^{1\times M}$ is the estimate of the displacement in $\boldsymbol{r}$ for all the M modal frequencies, and $\mathcal{N}$ is a fully connected multilayer perceptron (MLP) parametrized by $\mathbf{\Theta}$ that takes as input the spatial coordinates $\boldsymbol{r}$. The network is, thus designed to have M output channels, each corresponding to the displacement at a specific resonant frequency and for each input pair of spatial coordinates, the network predicts the displacement for all the M modes, providing a complete set of displacement values across all frequencies at each point.

Among the different MLP architectures that are available in the literature, we adopted the so-called SIREN [32] (see Fig. 1). As a matter of fact, SIREN proved to be an effective solution for providing implicit neural representation of several physical quantities, including images, audio, and the acoustic field. The structure of the adopted MLP is given as

$$\mathcal{N}(\mathbf{\Theta}, \mathbf{x}) = (\Phi_J \circ \Phi_{J-1} \circ \cdots \circ \Phi_1)(\mathbf{x}), \tag{5}$$

where $\mathbf{x}$ is the input of the network and the jth layer Φ_j adopts the sinusoidal function as nonlinear activation

$$\Phi_j(\mathbf{x}_j) = \sin\left(\omega_0 \mathbf{x}_j^T \mathbf{\Theta}_j + \mathbf{b}_j\right), \tag{6}$$

with $\mathbf{x}_j$, $\mathbf{\Theta}_j$, $\mathbf{b}_j$ are the jth input, weights and biases, respectively and ω_0 is an hyperparameter controlling the frequency of the sinusoidal function [32].

In this work, we employ a physics-informed SIREN in order to estimate the displacement. In practice, we replace the regularization term $\mathcal{R}$ in (3) with a physics-informed training in which the loss function contains a term implementing the PDE underlying the physical behaviour of the plate. Thus, the network aims at minimizing two distinct terms: a data-driven loss, which ensures that the predicted displacements match the observed data, and the physics-informed loss. The total loss is the sum of the two terms defined above, namely

$$\mathcal{L} = \lambda_d \left(\frac{1}{N_d} \sum_{i=1}^{N_d} ||\hat{\mathbf{w}}(\boldsymbol{r}_i) - \mathbf{w}(\boldsymbol{r}_i)||^2 \right) + \lambda_p \left(\frac{1}{N_c} \sum_{k=1}^{N_c} ||\mathcal{K}(\hat{\mathbf{w}}(\boldsymbol{r}_k))||^2 \right), \tag{7}$$

where N_d represents the number of known points, $\mathbf{w}(\boldsymbol{r}_i) \in \mathbb{C}^M \times 1$ is the vector of the known displacement in $\boldsymbol{r}_i$, $\hat{w}(\cdot)$ is the predicted displacement, and $\mathcal{K}(w)$ is the differential operator that represents the plate governing equation computed over N_c randomly generated points. Here, we adopted the as $\mathcal{K}(\cdot)$ the residual of the Kirchhoff plate equation that governs the beding vibration of a thin plate and defined for a frequency ω as [35]

$$D\nabla^4 w(x, y, \omega) - \rho h \omega^2 w(x, y, \omega) = 0, \quad \text{with} \quad D = \frac{Eh^3}{12(1-\nu^2)} \tag{8}$$

where D is the flexural rigidity of the plate, E is the Young's modulus, h the plate thickness, ν the Poisson's ratio, ∇^4 is the biharmonic operator, ρ is the material density and ω is the angular frequency at which the plate is vibrating. The physical loss acts as a regularization term, preventing overfitting and guiding the network towards a solution consistent with the expected behavior of a vibrating thin plate.

The weights λ_d and λ_p in the loss function (7) can be either fixed or are dynamically reweighted during training in order to avoid that one component shadows the other during the optimization. Here, we adopted the ReLoBRaLo algorithm [36] for the dynamic reweighting.

2.3 Nondimensionalization

As shown in [37], when the PDE coefficients differ significantly in magnitude, the loss landscape becomes more complex, making the optimization problem less prone to converge. This issue can be solved with the so-called *nondimensionalization*, a technique ensuring that all terms in the equations have similar order of magnitude. In order to perform the nondimensionalization of the Kirchhoff equation, characteristic scales for the spatial coordinates and frequency are introduced. In particular, the frequencies ω_m are normalized by the maximum resonance frequency $\omega_{\max}$ and the spatial variables $\boldsymbol{r} = (x, y)$ are scaled by a characteristic length scale L_{norm}, namely

$$L_{\text{norm}} = \sqrt[4]{\frac{D}{\rho h \omega_{\max}^2}}. \tag{9}$$

The result of such normalization is a set of dimensionless variables $\bar{x}$, $\bar{y}$, and $\bar{\omega}$, thus making the equation invariant to plate dimensions and frequency scaling. It follows that we can define the nondimensionalized form of the Kirchhoff equation (8) as

$$\frac{\partial^4 w}{\partial \bar{x}^4} + 2\frac{\partial^4 w}{\partial \bar{x}^2 \partial \bar{y}^2} + \frac{\partial^4 w}{\partial \bar{y}^4} = \bar{\omega}^2 w. \tag{10}$$

3. VALIDATION

The proposed PINN for the interpolation of modal displacement is implemented in Python using the PyTorch framework. Thus the network takes as input the normalized spatial coordinates $\bar{\boldsymbol{r}} = (\bar{x}, \bar{y}) \in \bar{\Omega}$. We adopted a shallow architecture that includes $J = 2$ hidden layers with 256 neurons each, using a sinusoidal activation function. The output layer consists of $M = 10$ neurons, corresponding to the first 10 resonant frequencies of the plate. A scheme of the network architecture is shown in Fig. 1.

We train the network with the Adam optimizer over 20000 epochs using a learning rate equals to 10^{-3}. The physics loss in (7) is computed over $N_c = 500$ randomly generated points. The dynamic weighting of the loss function is handled by the ReLoBRaLo algorithm, which adjusts the scaling factors λ_d and λ_p. The hyperparameters for ReLoBRaLo [36] are set as follows: $\alpha = 0.99$, $\rho = 0.999$, and $T = 10^{-3}$.

The data set of dispacement (1) has been obtained by means of FEA using the software COMSOL Multiphysics, simulating a thin rectangular plate. The plate is defined with dimensions of 20×35 cm, closely resembling those of a violin soundboard. The material properties were set to typical values for spruce wood, with a density of $420\,\frac{\text{kg}}{\text{m}^3}$, a Young's modulus of 10×10^6 Pa, and a Poisson's ratio of 0.28. An eigenfrequency study is conducted by assuming *free boundary conditions* and predicting the first ten plate natural vibration modes. The results of this study provided the transverse displacement values for a grid of 20×35 spatial points over the plate surface, with each point capturing the response in terms of displacement at each resonant frequency. A subset of these points was selected to simulate the limited experimental data available during training. We consider different number of available measurements, namely $N_d = [6, 8, 10, 12, 14, 16, 18]$ corresponding to a percentage of known points ranging within 1–2.5 %, approximately. The locations of these data points were generated randomly, following a uniform distribution. Finally, the displacement values were normalized between -1 and 1.

3.1 Metrics

To evaluate the model accuracy in the prediction of the displacement fields, we employed the Normalized Mean Squared Error (NMSE) defined as

$$\text{NMSE}(w^m, \hat{w}^m) = 20 \log_{10} \left(\frac{\frac{1}{N} \sum_{i=1}^{N} (w_i^m - \hat{w}_i^m)^2}{\frac{1}{N} \sum_{i=1}^{N} (w_i^m - \bar{w})^2} \right) \tag{11}$$

N is the number of points, and $\bar{w}$ represents the mean value of w.

3.2 Results

In order to provide a baseline for comparison, we implemented the Radial Basis Function (RBF) interpolation technique [33]. RBFs are commonly used for solving upsampling problems due to their ability to smoothly interpolate scattered data points. The method

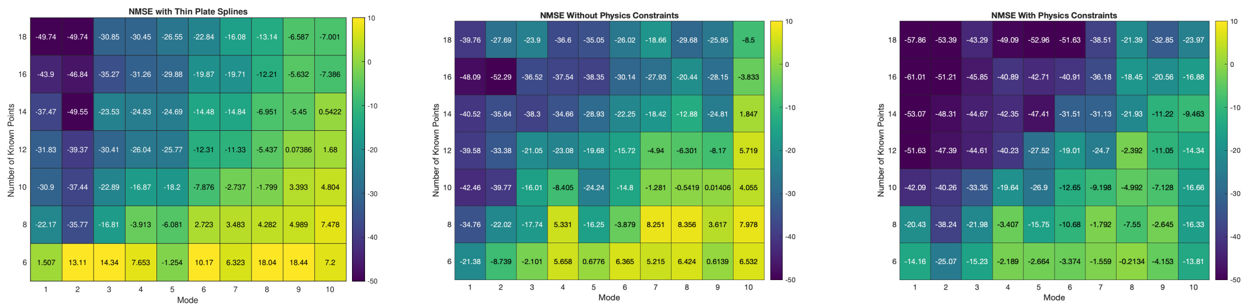

(a) (b) (c)

Figure 2. NMSE as a function of the mode and the number of known data points for each of the considered methods: **(a)** RBF interpolation using TPS, **(b)** purely data-driven NN and **(c)** PINN with physics-informed loss. NMSE values are reported in dB scale in the form of a heatmap, where high values are highlighted in yellow and low values are denoted with blue.

relies on a weighted sum of radial basis functions, which are centered at known data points. For this study, we employed the Thin Plate Spline (TPS) variant of RBF interpolation, which is particularly effective for solving mechanical deformation problems in plates [34, 38]. We used the `Rbf` function from the Python `scipy.interpolate` [1] library, specifying the `''thin plate''` radial basis function to perform the interpolation. The data points used in the RBF interpolation are the same as those employed for training the neural network.

To highlight the benefits of incorporating physical constraints, we then compare the PINN with a purely data-driven neural network. The network consists of the same architecture as the PINN, with the only changes being the absence of the governing equation loss and the use of the SiLU activation function. Without the physics-based loss, in fact, using the sine activation function led to significant overfitting. From now on, we will refer to this model as "NN".

Fig. 2(a) shows the NMSE heatmap for RBF interpolation using TPS, Fig. 2(b) displays the NMSE heatmap for the prediction of the NN and Fig. 2(c) the NMSE heatmap for the PINN results. The plots show results for the first ten vibration modes across varying numbers of known data points: 6, 8, 10, 12, 14, 16, and 18.

As expected, all methods perform well with a high number of data points, showing a clear improvement in accuracy as sufficient information is available. However, for very low numbers of data points, particularly under 10, both the RBF interpolation and the NN exhibit significantly higher NMSE values. In such cases, the models do not have enough data to generalize the vibrational behavior of the plate effectively, leading to poor predictions. The high NMSE values indicate that both methods are incapable of extrapolate any meaningful structure in the absence of sufficient data. In contrast, the PINN shows resilience in handling sparse data. The regularization provided by the physics-based constraints enables it to infer plausible solutions even in regions far from data points.

Fig. 3 compares the NMSE of the three different methods. The upper panel shows the mean NMSE across the number of data points for each mode, while the bottom panel shows the mean NMSE across modes for each number of data points, with error bars representing the corresponding standard deviation.

By inspecting the higher modes in Fig. 3 (top), it can be clearly noticed that both neural networks generally perform better than RBF for higher resonant frequencies. Regarding the dependence on the number of data points (Fig. 3, bottom), RBF and NN show comparable performances, while PINN stands out as the only approach showing a consistently decreasing trend in NMSE, directly correlated with the number of data points. To summarize, the results show that performance generally deteriorates as the number of known points decreases or as the mode number increases (i.e., higher frequencies). For sufficient data points and/or lower modes, all methods

[1] `https://docs.scipy.org/doc/scipy/reference/interpolate.html`

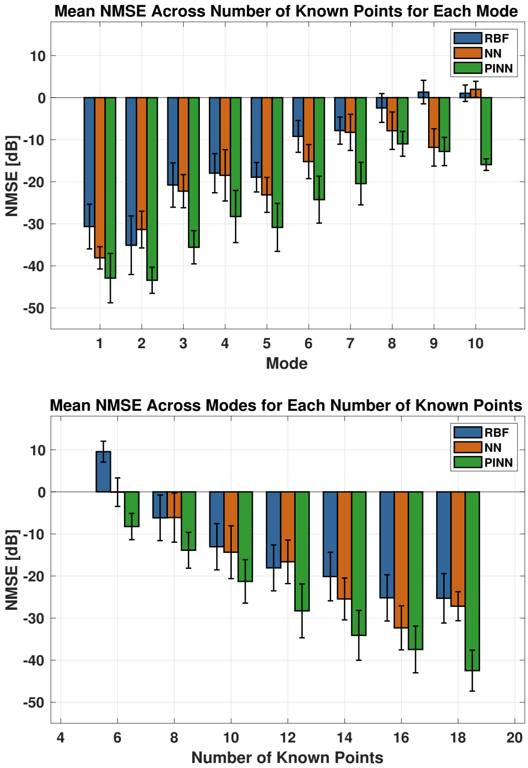

Figure 3. Comparison between the three different approaches: RBF interpolation with TPS (blue), NN (orange), and PINN (green). **Top:** mean NMSE across number of data points for each mode. **Bottom:** mean NMSE across modes for each number of data points (b). The black error bars denote the corresponding standard deviations.

perform well, with the PINN maintaining approximately 10 dB improvement over the baselines. However, what is particularly noteworthy is that, in cases with very few data points or higher frequencies, where the baselines produce completely incorrect predictions (positive NMSE), the PINN still manages to deliver meaningful and reliable solutions.

4. CONCLUSIONS

This work presents a PINN-based method for predicting the displacement field of a vibrating plate at resonance frequencies, leveraging physics-based constraints to improve accuracy and reduce dependency on extensive data. The method effectively upsamples sparse data to reconstruct continuous displacement fields, addressing challenges related to the spatial distribution and number of measurement points. The method was evaluated using COMSOL simulations, which demonstrated the robustness of the method, showing that the PINN consistently outperforms baseline approaches, namely RBF interpolation and purely data-driven NN. Indeed, while the baseline methods perform well with a large number of data points, their performance quickly decreases with lower data points. The PINN's ability to integrate physical laws into its loss function allows it to reconstruct the displacement field even in data-sparse regions. Similar approaches hold promise for applications in lutherie, where they could be valuable for tuning and analyzing the soundboard of musical instruments. More broadly, this study contributes to showcase the use of PINNs in structural mechanics, showing how these methods can solve mechanical problems governed by physical equations. Future improvements could involve further testing of the model with different geometries and materials, as well as refining the resolution for non-resonant frequencies by incorporating non-homogeneous Kirchhoff equations into the PINN.

5. ACKNOWLEDGMENTS

This work has been funded by “REPERTORIUM project. Grant agreement number 101095065. Horizon Europe. Cluster II. Culture, Creativity and Inclusive Society. Call HORIZON-CL2-2022-HERITAGE-01-02.”. This work was partially supported by the European Union - Next Generation EU under the Italian National Recovery and Resilience Plan (NRRP), Mission 4, Component 2, Investment 1.3, CUP D43C22003080001, partnership on ”Telecommunications of the Future” (PE00000001 - program “RESTART”)

6. REFERENCES

[1] R. Malvermi, M. Albano, S. Gonzalez, G. Fiocco, F. Antonacci, M. Malagodi, and A. Sarti, “The impact of alkaline treatments on elasticity in spruce tonewood,” *Scientific Reports*, vol. 12, no. 1, p. 13335, 2022.

[2] B. Schwarz and M. H. Richardson, “Experimental modal analysis,” in *Proceedings of CSI Reliability Week*, 1999.

[3] P. Avitabile, "Experimental modal analysis - a simple non-mathematical presentation," *Sound and Vibration*, vol. 35, pp. 20–31, 2001.

[4] A. Cunha and E. Caetano, "Experimental modal analysis of civil engineering structures," *Sound and Vibration*, vol. 40, 2006.

[5] M. Petyt, *Introduction to finite element vibration analysis*. Cambridge university press, 2010.

[6] L. L. Thompson, "A review of finite-element methods for time-harmonic acoustics," *The Journal of the Acoustical Society of America*, vol. 119, no. 3, pp. 1315–1330, 2006.

[7] J. D. Maynard, E. G. Williams, and Y. Lee, "Nearfield acoustic holography: I. theory of generalized holography and the development of NAH," *The Journal of the Acoustical Society of America*, vol. 78, no. 4, pp. 1395–1413, 1985.

[8] D. L. Donoho, "Compressed sensing," *IEEE Transactions on information theory*, vol. 52, no. 4, pp. 1289–1306, 2006.

[9] B. Schwarz, S. Richardson, and M. Richardson, "Curve fitting analytical mode shapes to experimental data," in *Topics in Modal Analysis & Testing, Volume 10*, pp. 45–59, Springer International Publishing, 2016.

[10] G. Chardon, A. Leblanc, and L. Daudet, "Plate impulse response spatial interpolation with sub-nyquist sampling," *Journal of Sound and Vibration*, vol. 330, pp. 5678–5689, 2011.

[11] S. Gonzalez, D. Salvi, D. Baeza, F. Antonacci, and A. Sarti, "A data-driven approach to violin making," *Scientific reports*, vol. 11, no. 1, p. 9455, 2021.

[12] D. G. Badiane, S. Gonzalez, R. Malvermi, F. Antonacci, and A. Sarti, "A neural network-based method for spruce tonewood characterization," *The Journal of the Acoustical Society of America*, vol. 154, pp. 730–738, 08 2023.

[13] M. Olivieri, R. Malvermi, M. Pezzoli, M. Zanoni, S. Gonzalez, F. Antonacci, and A. Sarti, "Audio information retrieval and musical acoustics," *IEEE Instrumentation & Measurement Magazine*, vol. 24, no. 7, pp. 10–20, 2021.

[14] J. C. Albarracín Sánchez, L. Comanducci, M. Pezzoli, and F. Antonacci, "Towards hrtf personalization using denoising diffusion models," in *ICASSP 2025 - 2025 IEEE International Conference on Acoustics, Speech and Signal Processing (ICASSP)*, pp. 1–5, 2025.

[15] A. Kaveh, *Applications of artificial neural networks and machine learning in civil engineering*. Springer, 2024.

[16] C. Campagnoli, M. Pezzoli, F. Antonacci, and A. Sarti, "Vibrational modal shape interpolation through convolutional auto encoder," in *INTER-NOISE and NOISE-CON Congress and Conference Proceedings*, vol. 261, pp. 5619–5626, Institute of Noise Control Engineering, 2020.

[17] M. Acerbi, R. Malvermi, M. Pezzoli, F. Antonacci, A. Sarti, and R. Corradi, "Interpolation of irregularly sampled frequency response functions using convolutional neural networks," in *ICASSP 2021-2021 IEEE International Conference on Acoustics, Speech and Signal Processing (ICASSP)*, pp. 950–954, IEEE, 2021.

[18] O. Ronneberger, P. Fischer, and T. Brox, "U-net: Convolutional networks for biomedical image segmentation," in *International Conference on Medical image computing and computer-assisted intervention*, pp. 234–241, Springer, 2015.

[19] R. Malvermi, F. Antonacci, A. Sarti, and R. Corradi, "Prediction of missing frequency response functions through deep image prior," in *2021 IEEE Workshop on Applications of Signal Processing to Audio and Acoustics (WASPAA)*, pp. 106–110, 2021.

[20] D. Ulyanov, A. Vedaldi, and V. Lempitsky, "Deep image prior," in *The IEEE Conference on Computer Vision and Pattern Recognition (CVPR)*, pp. 9446–9454, June 2018.

[21] M. Pezzoli, D. Perini, A. Bernardini, F. Borra, F. Antonacci, and A. Sarti, "Deep prior approach for room impulse response reconstruction," *Sensors*, vol. 22, no. 7, p. 2710, 2022.

[22] F. Miotello, M. Pezzoli, L. Comanducci, F. Antonacci, and A. Sarti, "Deep prior-based audio inpainting using multi-resolution harmonic convolutional neural networks," *IEEE/ACM Transactions on Audio, Speech, and Language Processing*, vol. 32, pp. 113–123, 2023.

[23] F. Kong, F. Picetti, V. Lipari, P. Bestagini, X. Tang, and S. Tubaro, "Deep prior-based unsupervised reconstruction of irregularly sampled seismic data," *IEEE Geoscience and Remote Sensing Letters*, vol. 19, pp. 1–5, 2020.

[24] M. Raissi, P. Perdikaris, and G. E. Karniadakis, "Physics-informed neural networks: A deep learning framework for solving forward and inverse problems involving nonlinear partial differential equations," *Journal of Computational physics*, vol. 378, pp. 686–707, 2019.

[25] E. Morena, R. Malvermi, M. Pezzoli, F. Antonacci, and A. Sarti, "Reconstruction of directional sources using physics-informed neural networks," in *INTER-NOISE and NOISE-CON Congress and Conference Proceedings*, vol. 270, pp. 6116–6126, Institute of Noise Control Engineering, 2024.

[26] M. Olivieri, M. Pezzoli, F. Antonacci, and A. Sarti, "A physics-informed neural network approach for nearfield acoustic holography," *Sensors*, vol. 21, no. 23, 2021.

[27] S. Koyama, J. G. Ribeiro, T. Nakamura, N. Ueno, and M. Pezzoli, "Physics-informed machine learning for sound field estimation: Fundamentals, state of the art, and challenges [special issue on model-based and data-driven audio signal processing]," *IEEE Signal Processing Magazine*, vol. 41, no. 6, pp. 60–71, 2025.

[28] X. Karakonstantis and E. Fernandez-Grande, "Room impulse response reconstuction using physics-constrained neural networks," *Forum Acusticum 2023*, 2023.

[29] M. Pezzoli, F. Antonacci, and A. Sarti, "Implicit neural representation with physics-informed neural networks for the reconstruction of the early part of room impulse responses," *Forum Acusticum 2023*, 2023.

[30] I. Tsunokuni, G. Sato, Y. Ikeda, and Y. Oikawa, "Spatial extrapolation of early room impulse responses with noise-robust physics-informed neural network," *IEICE Transactions on Fundamentals of Electronics, Communications and Computer Sciences*, vol. 107, no. 9, pp. 1556–1560, 2024.

[31] X. Luan, M. Olivieri, M. Pezzoli, F. Antonacci, and A. Sarti, "Complex-valued physics-informed neural network for near-field acoustic holography," in *2024 32nd European Signal Processing Conference (EUSIPCO)*, pp. 126–130, IEEE, 2024.

[32] V. Sitzmann, J. Martel, A. Bergman, D. Lindell, and G. Wetzstein, "Implicit neural representations with periodic activation functions," *Advances in neural information processing systems*, vol. 33, pp. 7462–7473, 2020.

[33] F. Bookstein, "Principal warps: thin-plate splines and the decomposition of deformations," *IEEE Transactions on Pattern Analysis and Machine Intelligence*, vol. 11, no. 6, pp. 567–585, 1989.

[34] G. Donato and S. Belongie, "Approximate thin plate spline mappings," in *Computer Vision — ECCV 2002*, pp. 21–31, Springer Berlin Heidelberg, 2002.

[35] A. W. Leissa, "The free vibration of rectangular plate," *Journal of Sound and Vibration*, 1973.

[36] R. Bischof and M. A. Kraus, "Multi-objective loss balancing for physics-informed deep learning," *Computer Methods in Applied Mechanics and Engineering*, vol. 439, p. 117914, 2025.

[37] A. Krishnapriyan, A. Gholami, S. Zhe, R. Kirby, and M. W. Mahoney, "Characterizing possible failure modes in physics-informed neural networks," *Advances in neural information processing systems*, vol. 34, pp. 26548–26560, 2021.

[38] W. Keller and A. Borkowski, "Thin plate spline interpolation," *Journal of Geodesy*, vol. 93, pp. 1251–1269, 2019.